
**Supramolecular Chemistry**
Publication details, including instructions for authors and subscription information:
http://www.informaworld.com/smpp/title~content=t713649759

# Flip-flop Motion of Circular Hydrogen Bond Array in Thiacalix[4]arene

Jan Lang[a]; Kateřina Vágnerová[a]; Jiří Czernek[b]; Pavel Lhoták[c]
[a] Department of Low Temperature Physics, Faculty of Mathematics and Physics, Charles University, Prague 8, Czech Republic [b] Institute of Macromolecular Chemistry, Academy of Sciences of the Czech Republic, Prague 6, Czech Republic [c] Department of Organic Chemistry, Institute of Chemical Technology, Prague 6, Czech Republic

**To cite this Article** Lang, Jan , Vágnerová, Kateřina , Czernek, Jiří and Lhoták, Pavel(2006) 'Flip-flop Motion of Circular Hydrogen Bond Array in Thiacalix[4]arene', Supramolecular Chemistry, 18: 4, 371 — 381
**To link to this Article: DOI:** 10.1080/10610270600650790
**URL:** http://dx.doi.org/10.1080/10610270600650790

*Supramolecular Chemistry*, June 2006 Vol. 18 (4), pp. 371–381

Taylor & Francis
Taylor & Francis Group

# Flip–flop Motion of Circular Hydrogen Bond Array in Thiacalix[4]arene

JAN LANG[a,b,*], KATEŘINA VÁGNEROVÁ[b], JIŘÍ CZERNEK[c] and PAVEL LHOTÁK[d]

[a]*Laboratory of NMR Spectroscopy, Institute of Chemical Technology, Technická 5, CZ-166 28 Prague 6, Czech Republic;* [b]*Department of Low Temperature Physics, Faculty of Mathematics and Physics, Charles University, V Holešovickách 2, CZ-180 00 Prague 8, Czech Republic;* [c]*Institute of Macromolecular Chemistry, Academy of Sciences of the Czech Republic, Heyrovský Square 2, CZ-161 37 Prague 6, Czech Republic;* [d]*Department of Organic Chemistry, Institute of Chemical Technology, Technická 5, CZ-166 28 Prague 6, Czech Republic*

*(Received 23 December 2005; Accepted 17 February 2006)*



**Thiacalix[4]arene contains a circular array of four equivalent hydrogen bonds on its lower rim. The array undergoes a flip–flop motion between two possible directions. The rate of this motion in the temperature range 223–313 K is assessed by means of measurements of the nuclear spin relaxation. The values of the activation enthalpy (38.7 kJ mol$^{-1}$) and of the activation entropy (−15 J mol$^{-1}$ K$^{-1}$) were determined. In addition, correlation times of molecular tumbling have been determined in the same temperature range. The measured properties of thiacalix[4]arene are compared to those of the "classical" calix[4]arene in order to utilize them for fine tuning of the building blocks in supramolecular chemistry.**

*Keywords*: Flip–flop motion; Hydrogen bond; Enthalpy; Entropy; NMR, *ab initio* calculation; Calix[4]arene

## INTRODUCTION

Calix[4]arenes have been widely accepted as one of fundamental structural motifs in supramolecular chemistry due to their favorable properties such as easy synthesis, derivatization potential, and ability to form various complexes and adducts thanks to pre-organization of their cavity (Fig. 1) [1,2].

The cavity can, in principle, adopt four basic structures—*cone*, *partial cone*, *1,2-alternate* and *1,3-alternate*. Interconversion between the conformers is possible provided that the lower rim substituent is sufficiently small to pass through the annulus of the cavity [3,4]. However, if the lower rim substituent groups take part in some specific interaction, certain conformations may be thermodynamically favored or disfavored. This is the case in tetrahydroxycalix[4]arene and tetrahydroxythiacalix[4]arene ("tetrahydroxy" prefix is further omitted), whose hydroxyl groups form a circular array of four hydrogen bonds that stabilizes the conical shape, and disfavors other conformations forming a smaller number of hydrogen bonds [5]. However, if some of the hydrogen bonds are broken, the phenyl rings are allowed to rotate forming the identical conical structure turned "inside out" (*cone–inverted cone* transition) [3,6,7].

The hydrogen bonding array in calix[4]arenes is quite exclusive in several aspects. It is responsible for stabilization of geometry of the calix[4]arene cavity (of course, besides the covalent bonds involved in the calix[4]arene macrocycle). Consequently, changes induced specifically to the properties of the hydrogen bonds can be utilized in fine-tuning of the cavity geometry and the rigidity of the system.

Other important aspect of the calix[4]arene hydrogen bond array properties is the high degree of symmetry making all the four hydrogen bonds identical. Therefore, it can be used as a model system for other more extensive hydrogen bonding networks where it is not possible to detect selectively properties of one particular hydrogen bond, and rather an average behavior of a number of different hydrogen bonds is observed. This relates, for instance, to hydrogen bonding networks formed in water, alcohols, other hydrophilic solvents and also in less symmetrical macrocyclic compounds such as cyclodextrins.

Most recently, we have published a method to detect the rate of inversion of the sense of hydrogen bond array in calix[4]arene by means of the measurements of

*Corresponding author. Tel: + 420 220443805. Fax: + 420 24311082. E-mail: jan.lang@vscht.cz

ISSN 1061-0278 print/ISSN 1029-0478 online © 2006 Taylor & Francis
DOI: 10.1080/10610270600650790

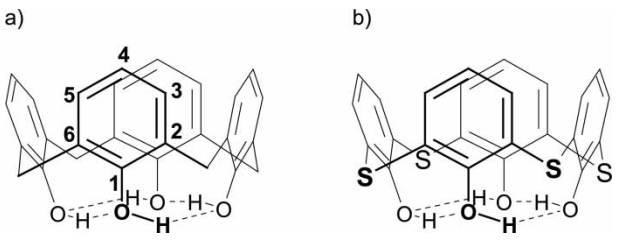


FIGURE 1 Calix[4]arene (a) and thiacalix[4]arene (b) with the numbering of carbon atoms adopted in this work.

the transverse $^{13}C$ nuclear spin relaxation. It allowed us to determine the activation enthalpy and entropy of the flip–flop motion that was found uncorrelated with other modes of molecular motions present: molecular tumbling and the *cone–inverted cone* transition [8].

In this paper, we report on the determination of the activation parameters of the hydrogen bond array reversal in thiacalix[4]arene in a non-polar solution. Thiacalix[4]arene [9–11] is a structural analog of the "classical" calix[4]arene with the methylene bridges between the phenyl rings replaced by sulfur atoms. The structural and dynamical properties of calix[4]arene and thiacalix[4]arene are compared in connection with the determined hydrogen bonds characteristics.



## THEORETICAL PART

### Nuclear Spin Relaxation in Thiacalix[4]arene

In this work, the nuclear spin relaxation is used as a main tool to assess the dynamic behavior. There are two main sources of the $^{13}C$ relaxation in thiacalix[4]arene: the magnetic dipole–dipole (DD) interaction between $^{13}C$ and $^{1}H$ nuclei and the anisotropy of the $^{13}C$ chemical shift (CSA).

$^{13}C$ nuclear spins bearing directly bonded hydrogen atoms relax predominantly due to the DD interaction with protons attached to them. Contributions of this mechanism to relaxation rates are denoted as $R_1^{DD}$ (longitudinal) and $R_2^{DD}$ (transverse). In addition, the $^{13}C-\{^{1}H\}$ heteronuclear Overhauser enhancement, which is related to the cross-relaxation rate $\sigma^{DD}$, is commonly measured [12].

The amplitude factor of the interaction is the dipole–dipole coupling constant. It is inversely proportional to the sixth power of the distance between the interacting nuclei. The value of 21.5 kHz was found appropriate previously for the directly bonded $^{13}C-^{1}H$ pair [13].

Especially for nuclei without directly bonded hydrogens, the long range interaction with other protons in the molecule may not be negligible. Therefore, a correction for the long range interaction is performed in the way that all the pair-wise DD coupling constants for a $^{13}C$ nucleus of interest are summed up (based on the interatomic distances taken from the *ab initio* optimized structure) and used as a single effective value of the DD coupling constant.

Since all the carbon atoms in thiacalix[4]arene are involved in aromatic moieties, the relaxation due to the chemical shift anisotropy (CSA) is also quite important. The corresponding contributions to the rates are denoted as $R_1^{CSA}$ (longitudinal) and $R_2^{CSA}$ (transverse) [12].

We do not consider an interference of the two relaxation mechanisms because the experiments are designed to suppress it. The measured relaxation rates $R_1$ and $R_2$ are thus sums of the two contributions (Eqs. (1) and (2)).

$$R_1 = R_1^{DD} + R_1^{CSA} \tag{1}$$

$$R_2 = R_2^{DD} + R_2^{CSA} \tag{2}$$

The heteronuclear steady state NOE in the presence of CSA is expressed according to Eq. (3) ($\gamma_H$, $\gamma_C$ are magnetogyric ratios of $^{1}H$ and $^{13}C$ nuclei, $N_H$ is a number of directly bound hydrogen atoms [12].

$$\mathrm{NOE} = 1 + \left(\frac{\gamma_H}{\gamma_C}\right)\frac{N_H\sigma^{DD}}{R_1^{DD} + R_1^{CSA}} \tag{3}$$

The relaxation rates defined above are related to the products of the corresponding interaction constants (DD coupling constant and effective CSA, $CSA_{eff}$) and to the autocorrelated spectral densities $J(\omega)$, describing the stochastic molecular rotational motions modulating the DD interactions and CSA [12]. Definitions of tensorial components $\delta_{11}$, $\delta_{22}$, $\delta_{33}$, of the chemical shift tensor (CST), its anisotropy $\Delta\sigma$, asymmetry $\eta$ and a complete set of the used equations together with their more thorough discussion can be found in our previous work [8].

Expression for the spectral densities $J(\omega)$ is derived according to the presumed type of molecular rotational motions. Since the calix[4]arene molecule was previously found internally rigid [13–15], and its shape is rather compact, the simple model of the rigid body isotropic reorientation is the first option to use. The tumbling of the whole molecule is described by a single parameter, the correlation time $\tau_M$. The spectral densities $J(\omega)$ derived for this model have a Lorentzian form expressed by Eq. (4) [12].

$$J(\omega) = \frac{2}{5}\left(\frac{\tau_M}{1+\omega^2\tau_M^2}\right) \tag{4}$$

If the chemical exchange that is fast with respect to the chemical shifts of the exchanging nuclei occurs at a certain resonance, it contributes to its transverse relaxation rate (Eq. (5)).

$$R_2 = R_2^{DD} + R_2^{CSA} + R_2^{ex} \tag{5}$$

The exchange term $R_2^{ex}$ depends on the amplitude of the applied radiofrequency field as derived by Luz

and Meiboom [16]. When the transverse relaxation is measured using the multiple echo Carr–Purcell–Meiboom–Gill (CPMG) pulse sequence (the total number of echoes in the sequence is denoted $n$) [17,18], the effective radiofrequency field strength can be modified by changing the echo-time $t_{echo}$ (the delay between two subsequent $^{13}C$ $\pi$-pulses in the CPMG sequence). The exchange contribution then depends on the echo-time according to Eq. (6).

$$R_2^{ex} = p_A p_B (\Delta\omega)^2 \tau_{ex} \left[1 - \frac{2\tau_{ex}}{t_{echo}} \tanh\left(\frac{t_{echo}}{2\tau_{ex}}\right)\right] \quad (6)$$

$p_A$, $p_B$ are populations of exchanging sites, $\Delta\omega$ is the chemical shift difference of the exchanging resonances, $\tau_{ex}$ is the correlation time of the chemical exchange ($k_{ex} = 1/\tau_{ex}$ is the chemical exchange rate).

In the chemical kinetics terms, the hydrogen bond reversal is a symmetrical first order reaction A ↔ B, i.e. $p_A = p_B = 0.5$, and the reaction rate constant $k$ is related to the chemical exchange rate as: $k = k_{ex}/2$.

The peak intensity in the CPMG experiment is thus expressed by Eq. (7):

$$I(t) = I_0 \exp\left[-\left(R_2^{DD} + R_2^{CSA}\right) n t_{echo}\right] \exp\left(-R_2^{ex} n t_{echo}\right) \quad (7)$$

In order to measure the transverse relaxation in absence of the chemical exchange, the experiment is commonly repeated several times with increasing number of repetitions of the spin echo segment $n$, keeping the echo-time constant $t_{echo}$ constant (typically at 0.8 ms). In order to determine the chemical exchange parameters ($\Delta\omega$, $\tau_{ex}$), the measurements at variable $t_{echo}$ must be added.

It is therefore necessary to measure the spectral intensity dependence on the both variables: $n$ and $t_{echo}$. Traditionally (and also in our previous work), this has been achieved by several measurements of $R_2$ at different values of $t_{echo}$. Thus, each $R_2$ value is obtained from an experiment with $n$ incremented. The next experiment is performed in a similar way for a new value of $t_{echo}$, and so forth. This approach was found too time consuming in this case. Hence, the "accelerated" approach suggested by Ishima and coworkers [19] was applied: $n$ and $t_{echo}$ are incremented/decremented synchronously so that $nt_{echo}$ = const. (20, 30 or 100 ms in this work).

## RESULTS AND DISCUSSION

### $^{13}C$ and $^{1}H$ NMR Spectra

$^{13}C$ spectrum of thiacalix[4]arene (Fig. 3) acquired at temperature higher than 243 K contains four lines that were assigned by ordinary homonuclear $^{1}H$, $^{13}C$ and a heterocorrelated $^{1}H$, $^{13}C$-HMQC experiments. When cooling the sample down, a significant

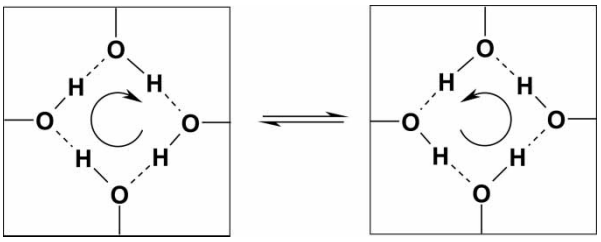

FIGURE 2 Schematic drawing of the flip–flop movement of the array of hydrogen bonds on the lower rim of calix[4]arene or thiacalix[4]arene.

selective broadening and even splitting (below 213 K) occur for the line corresponding to C-2, C-6, and, to a lesser extent, C-3, C-5. This effect is a result of the flip–flop motion of the lower rim hydrogen bond array. The pairs C-2, C-6 and C-3, C-5 become chemically non-equivalent due to the two possible orientations of the hydroxyl groups (see Fig. 2).

The rate of the chemical exchange could be estimated from the broadening of the spectral lines, however, in practice, when the spectra contain substantial amount of noise, the measurements of the transverse spin relaxation are much more accurate. Here we only note that the splitting of the signals corresponding to C-2 and C-6 at 203 K and 193 K is 128.3 Hz (at magnetic field of 11.7 T).

$^{1}H$ spectrum of thiacalix[4]arene is very simple, consisting of a triplet of H-4, a doublet of H-3, H-5 and a singlet of hydroxyl group (the chemical shifts at 303 K are: 6.79, 7.64, and 9.51 ppm, respectively). Upon cooling no differential behavior is observed for the resonances of H-3, H-5 and H-4. This means that the chemical shifts of H-3, H-5 are, even at the lowest achievable temperatures, averaged by the chemical exchange, which is therefore fast on the $^{1}H$ chemical shift timescale at 11.7 T. In contrary, the temperature dependence was observed for hydroxyl group chemical shift: its value changes from 9.62 ppm (193 K) to 9.49 ppm (313 K). This is a consequence of

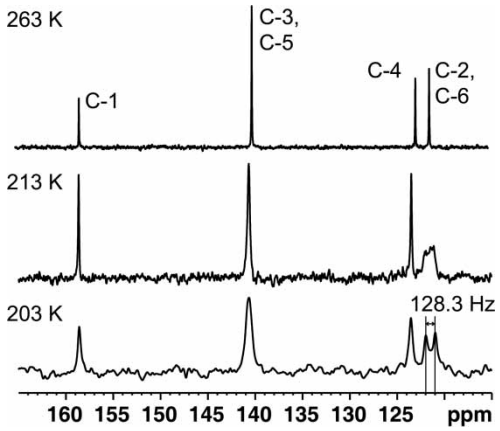


FIGURE 3 The $^{13}C$ spectra of thiacalix[4]arene at 263 K, 213 K and 203 K with the assignment. The broadening and splitting of C-2, C-6 peak at low-temperatures is documented.

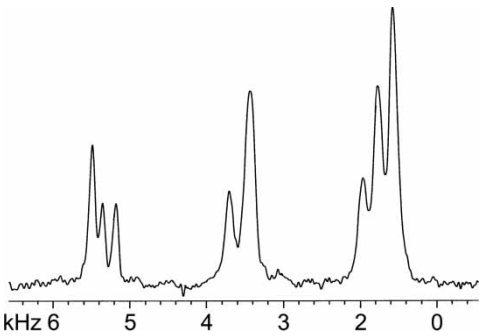


FIGURE 4 The isotropic part of the $^{13}C$ NMR spectrum of thiacalix[4]arene in the solid state measured at 9.4 T and 233 K.

decreasing stability of hydrogen bonds with increasing temperature.

An accurate determination of molecular motions relies on the knowledge of amplitudes of interactions responsible for the relaxation, namely the DD coupling constants and the effective chemical shift anisotropies ($CSA_{eff}$). While the first one is inversely proportional to the sixth power of the distance between the two interacting nuclei, with the distances having been acceptably well established (for further discussion see refs. [13,20]), the latter ones need to be determined. The elegant method is the measurement of the principal components of the $^{13}C$ CST by means of 2D PASS solid state NMR pulse sequence [21]. We carried out this experiment at the temperature of 233 K in order to suppress a possibility of local molecular motions in the solid state that could partially average out the anisotropy of the chemical shielding tensor (CST). The isotropic part of the $^{13}C$ 2D PASS solid state spectrum is shown in Fig. 4. The apparent $C_4$ symmetry in the liquid state spectrum is not retained in the solid state where each resonance becomes split to several spectral lines. Therefore, the lines corresponding to C-2, C-6 and to C-4 suffer a total overlap. The Herzberg–Berger analysis of intensities of rotational sidebands [22] providing the CST components is only possible for the resonances of C-1 and C-3, C-5, and thus the set of the measured $CSA_{eff}$ values remains incomplete (see Table I).

TABLE I The principal components of the $^{13}C$ CST determined experimentally by means of the 2D PASS solid state NMR pulse sequence. The chemical shifts $\delta_{exptl}$ determined in the liquid state at 233 K were used as the values of isotropic chemical shifts for scaling of the principal components. The values for C-2, C-6 and C-4 could not be determined due to an overlap in the solid state spectrum.

| Nucleus | $\delta_{exp}$ | $\delta_{11}$ | $\delta_{22}$ | $\delta_{33}$ | $\Delta\sigma$ | $\eta$ | $CSA_{eff}$ |
|---|---|---|---|---|---|---|---|
| C-1 | 156.92 | 241 | 167 | 63 | −140.6 | 0.7931 | 154.6 |
| C-2, C-6 | 119.85 | – | – | – | – | – | – |
| C-3,C-5 | 138.82 | 232 | 151 | 33 | −158.5 | 0.7643 | 173.3 |
| C-4 | 121.60 | – | – | – | – | – | – |

### *Ab Initio* Calculations

An alternative method to determine the principle components of the CST is to perform an *ab initio* quantum chemical calculation [23]. We successfully applied this approach to the "classical" calix[4]arene [8], and the same strategy was employed here (see the Methods section for details). Namely, first the geometry of thiacalix[4]arene was optimized using the density functional theory (DFT)-based B3LYP/6-31G** method. Subsequently the $^{13}C$ CSTs were obtained using the SOS–DFPT–IGLO method and employing the IGLO-III basis set. This strategy was shown to reliably describe the $^{13}C$ chemical shielding in numerous organic systems [24] and provided the description of the CSTs crucial for an interpretation of the experimental relaxation data [25,26]. It yielded values fairly close to the measured results also in the present case of thiacalix[4]arene (see Tables I and II). For example, the calculated chemical shielding anisotropies differ only up to 4.5 ppm (in the case of the C-1 nucleus) from their known experimental counterparts. Consequently, the DFT strategy employed can be considered to be sufficiently accurate for the purpose of this investigation.

### Nuclear Spin Relaxation

The determined temperature dependences of the $^{13}C$ longitudinal relaxation rates $R_1$, $^{13}C-\{^1H\}$ heteronuclear Overhauser effect (NOE) and $^{13}C$ transverse relaxation rates $R_2$ are shown in Figs. 5–7 (the corresponding tables can be found in Supplementary Material [28]). The longitudinal relaxation rates $R_1$ (Fig. 5) have maximum at 233 K, which agrees well with the classical figure with the maximum corresponding to the transition of molecular tumbling towards the extreme narrowing regime. The rates for the C-3, C-5 and C-4 nuclei are similar to

TABLE II The DFT-computed chemical shift data and the experimental values of the $^{13}C$ chemical shift (all values are in ppm). The DFT-computed principal components $\sigma_{11}$, $\sigma_{22}$ and $\sigma_{33}$ of the CST were converted into the principal components $\delta_{11}$, $\delta_{22}$ and $\delta_{33}$ of the CST by using the relationship $\delta_{ii} = 186.4 - \sigma_{ii}$, where 186.4 ppm is the experimental chemical shielding of gaseous tetramethylsilane in the zero-pressure limit [27]. $\Delta\sigma$ and $\eta$ are the anisotropy and the asymmetry of the CST that determine $CSA_{eff}$, the amplitude factor of the CSA relaxation mechanism. The averages of $CSA_{eff}$ of C-2, C-6 and C-3, C-5 (134.0 and 181.1 ppm, respectively) were used for the evaluation of the liquid state spin relaxation.

| Nucleus | $\delta_{11}$ | $\delta_{22}$ | $\delta_{33}$ | $\Delta\sigma$ | $\eta$ | $CSA_{eff}$ |
|---|---|---|---|---|---|---|
| C-1 | 257 | 180 | 74 | −145.1 | 0.7900 | 159.4 |
| C-2 | 205 | 154 | 51 | −128.3 | 0.5864 | 135.5 |
| C-3 | 251 | 153 | 42 | −160.5 | 0.9121 | 181.4 |
| C-4 | 231 | 134 | 17 | −165.6 | 0.8758 | 185.6 |
| C-5 | 251 | 153 | 42 | −159.9 | 0.9135 | 180.8 |
| C-6 | 204 | 154 | 53 | −125.3 | 0.6004 | 132.6 |

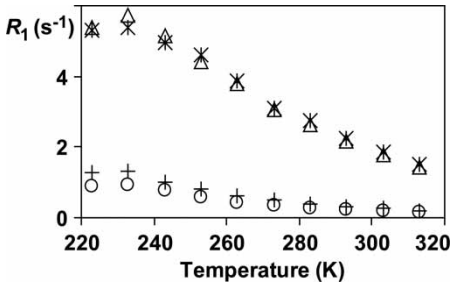


FIGURE 5 The temperature dependence of the measured $^{13}$C longitudinal relaxation rates $R_1$ in thiacalix[4]arene: C-1 ( + ), C-2, C-6 (○), C-3, C-5 (Δ), C-4 (*).

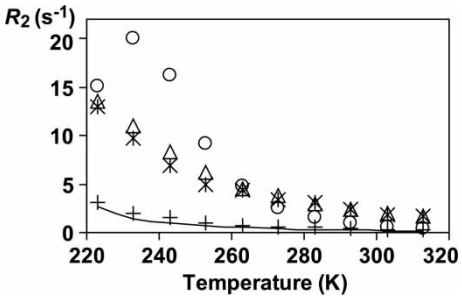


FIGURE 7 The temperature dependence of the measured $^{13}$C transverse relaxation rates $R_2$ in thiacalix[4]arene: C-1 (cross), C-2, C-6 (circle), C-3, C-5 (Δ), C-4 (star). The solid line displays the calculated values of the relaxation rate of C-2, C-6 without the contribution of the chemical exchange.

each other, and they are considerably higher than those of C-1 and C-2, C-6. This is because, the first group relaxes mainly due to the DD interaction with the directly bound hydrogen nucleus, and to a lesser extent also due to CSA mechanism. The latter group of nuclei is relaxed almost exclusively by CSA, which is, however, a less efficient mechanism.

The NOE at all $^{13}$C nuclei increases with temperature (see Fig. 6). Since it reflects the ratio of DD and CSA mechanisms, it is larger for C-3, C-5 and C-4 nuclei, although it does not reach its theoretical maximum of 3, when the relaxation is caused exclusively by $^{13}$C–$^{1}$H DD interaction. The NOE value just a little over 1.0 is consistent with the dominance of the CSA mechanism for C-1 and C-2, C-6, with only a small contribution of the long-range DD interactions with hydrogen nuclei in the molecule.

The temperature dependence of the transverse relaxation rates $R_2$ (Fig. 7) should be monotonically dropping with increasing temperature. This is the case for the C-1 and C-4 nuclei (the absolute difference between their relaxation rates is caused by the difference in strengths of the two interactions, as explained above for the case of the longitudinal relaxation), but there is a clear hump in the temperature dependence for C-2, C-6, and the calculation (*vide infra*) confirms the existence of small enhancements to the transverse rate of C-3, C-5 as well. Enhancements of the transverse relaxation of C-2, C-6 and C-3, C-5 is another representation of the differential broadening of their spectral lines observed in the basic $^{13}$C spectra. The extra contribution to the transverse relaxation is the effect of chemical exchange. The best way how to separate this contribution is to adopt all exchange-unaffected experimental relaxation parameters ($R_1$ and NOE of all nuclei and $R_2$ of C-1 and C-4) and calculate the "exchange-free" theoretical transverse relaxation rates of C-2, C-6 and C-3, C-5. This is achieved through the calculation of the parameters of molecular tumbling as described in the theoretical part.

The correlation times resulting from the motional analysis are shown in Table III and Fig. 8. The temperature dependence follows the Arrhenius form with the activation energy of 17.7 kJ mol$^{-1}$ (± 0.2 kJ mol$^{-1}$) and the preexponential factor of 79 fs (± 8 fs). These values were obtained after removal of the data point established for the lowest measured temperature (223 K). The reason of its deviation from the Arrhenius behavior may lie in an inadequacy of the motional model. It is possible that certain modes of the molecular motions become hindered at low-temperatures, and hence the motion is not fully isotropic anymore. Except of this one point, the values follow the Arrhenius dependence very well (for further discussion, see part *Comparison with Calix[4]arenes and Calix[6]arenes*).

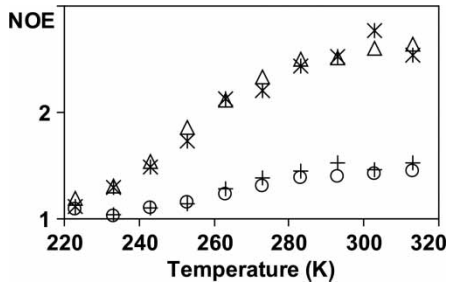


FIGURE 6 The temperature dependence of the measured {$^{1}$H}-$^{13}$C nuclear Overhauser enhancement (NOE) in thiacalix[4]arene: C-1 (cross), C-2, C-6 (circle), C-3, C-5 (Δ), C-4 (star).

TABLE III Temperature dependence of the determined global correlation times $\tau_M$ of molecular tumbling and their standard errors $\delta\tau_M$.

| $T$/K | $\tau_M$/ns | $\delta\tau_M$/ns |
|---|---|---|
| 223 | 1.91 | 0.12 |
| 233 | 0.763 | 0.069 |
| 243 | 0.501 | 0.024 |
| 253 | 0.344 | 0.013 |
| 263 | 0.246 | 0.008 |
| 273 | 0.183 | 0.006 |
| 283 | 0.145 | 0.004 |
| 293 | 0.114 | 0.003 |
| 303 | 0.089 | 0.02 |
| 313 | 0.072 | 0.02 |

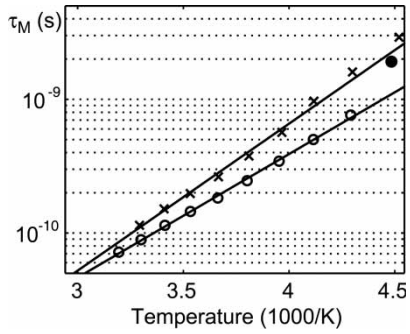


FIGURE 8 The temperature dependence of the correlation time $\tau_M$ of the isotropic reorientation determined for calix[4]arene × (Ref. [8]) and thiacalix[4]arene (○) together with the fitted Arrhenius dependences. The value excluded from the fit is marked as (●).

The computational routine used for the calculation of motional parameters provided also the theoretical values of transverse relaxation rates ($R_2^{DD} + R_2^{CSA}$) of C-2, C-6. The difference between the theoretical and the measured rates of C-2, C-6 accounts for the substantial chemical exchange contribution (Fig. 7: compare the solid line with the circle marks). These values were entered into Eq. (7) to obtain the chemical exchange parameters.

## Chemical Exchange

As mentioned above, the flip–flop motion of hydrogen bond array affects the transverse relaxation of carbons C-2, C-6 and C-3, C-5. The latter pair is affected only marginally and therefore only the substantially enhanced C-2, C-6 transverse relaxation was used to quantify the exchange processes.

The typical experimental data obtained from the two methods of sampling the surface of the peak amplitudes dependence on the echo-time $t_{echo}$ and number of the echo repetitions $n$ are shown in Figs. 9 and 10. The complete set of the experimental signal intensities is available as Supplementary Material [28]. The conventional approach (Fig. 9) consists of several measurements of the transverse relaxation rates performed with different settings of the echo-times. This method was employed for the measurements at 223 K. The second "accelerated" method (Fig. 10) consists of a single measurement of $T_2$ with $t_{echo} = 0.8$ ms (the experiment needed for determination of molecular tumbling) and two experiments with the $nt_{echo}$ products constant (20 and 30 ms). We developed a routine in Matlab 6 for iterative fitting of chemical exchange parameters simultaneously from all experimental signal intensities at a particular temperature by means of Eq. (7) (for the results see Table IV). Thus, the mathematical treatment is the same for the two experimental approaches. The "accelerated" approach allows for a measurement of the chemical exchange in less experimental time at the cost of certain loss of precision. However, the error analysis showed that

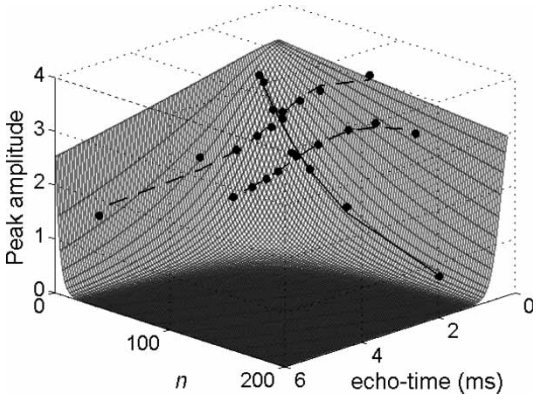


FIGURE 10 Peak intensities of C-2, C-6 from the transverse relaxation experiments at 233 K dependent on the echo-time $t_{echo}$ and the number of echoes $n$. The surface and the lines are the best fit according to Eqs. (6) and (7). The lines are connecting the points from individual experiments, namely, a single CPMG experiments at the fixed echo-time 0.8 ms (solid line) and two "accelerated" experiments with $nt_{echo}$ equal to 20 and 30 ms (dashed lines).

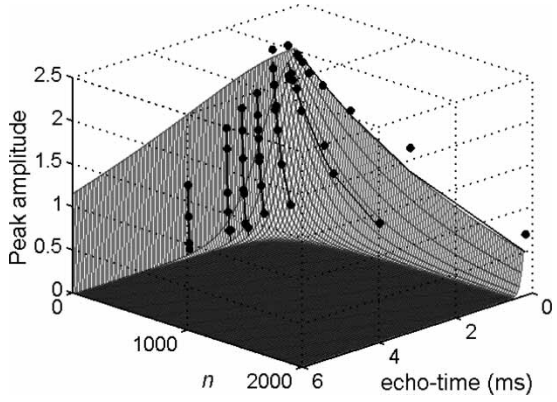


FIGURE 9 Peak amplitudes of C-2, C-6 from the transverse relaxation experiments at 223 K dependent on the echo-time $t_{echo}$ and the number of echoes $n$. The surface and the lines are the best fits according to Eqs. (6) and (7). The lines are connecting the points from the same experiments, namely, the CPMG experiments at the fixed echo-times.

TABLE IV The determined temperature ($T$) dependence of the parameters of the hydrogen bonds array flip–flop: the chemical shift difference $\Delta\omega$ (expressed in Hz), the chemical exchange correlation time $\tau_{ex}$, its standard error $\delta\tau_{ex}$, the chemical exchange rate $k$ and the activation free energy $\Delta G$. The standard errors are 2 Hz and 0.1 kJ mol$^{-1}$ for $\Delta\omega$ and $\Delta G$, respectively.

| $T$/K | $(\Delta\omega/2\pi)$/ Hz | $\tau_{ex}$ /μs | $\delta\tau_{ex}$/μs | $k$/(1000/s) | $\Delta G$/ (kJmol$^{-1}$) |
|---|---|---|---|---|---|
| 223 | 131 | 690 | 60 | 0.727 | 42.0 |
| 233 | 134 | 293 | 25 | 1.71 | 42.2 |
| 243 | 138 | 112 | 8 | 4.46 | 42.3 |
| 253 | 134† | 48 | 6 | 10.4 | 42.5 |
| 263 | 134† | 27.3 | 1.2 | 18.3 | 42.6 |
| 273 | 134† | 13.4 | 0.3 | 37.3 | 42.8 |
| 283 | 134† | 7.3 | 0.2 | 68.4 | 42.9 |
| 293 | 134† | 3.9 | 0.2 | 128 | 43.1 |
| 303 | 134† | 2.0 | 0.1 | 253 | 43.2 |
| 313 | 134† | 1.06 | 0.08 | 471 | 43.4 |

† A fixed value of $\Delta\omega$ (the average of the values corresponding to the 223–243 K temperature range) was used in the calculations.

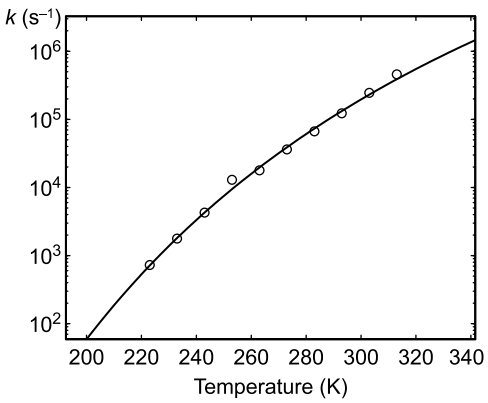


FIGURE 11 The temperature dependence of the hydrogen bond array flip–flop rate constants. The solid line is the best fit to the Eyring equation ($\Delta H = 38.7\,\mathrm{kJ\,mol^{-1}}$, $\Delta S = -15\,\mathrm{Jmol^{-1}K^{-1}}$). Estimated standard errors of $\Delta H$ and $\Delta S$ are $0.7\,\mathrm{kJ\,mol^{-1}}$ and $3\,\mathrm{J\,mol^{-1}\,K^{-1}}$, respectively.

the error of the determined correlation times of the chemical exchange did not increase substantially (see Table IV).

At temperatures higher than 243 K, the chemical exchange contribution to relaxation becomes independent of the echo-time, although still significantly enhancing the relaxation rates. Here, it is not possible to determine two independent variables ($\Delta\omega$, $t_{echo}$), and therefore the value of $\Delta\omega$ was set to 134.4 Hz, the average from the measurements in the 223–243 K range, and only $t_{echo}$ was fitted. This average value of $\Delta\omega$ agrees well with the value of 128.3 Hz read directly from the splitting of the C-2, C-6 signal in the $^{13}C$ spectrum at 203 K.

The temperature dependence of the chemical exchange rate can be approximated by means of Eyring equation with two parameters: the activation enthalpy $\Delta H$ and the activation entropy $\Delta S$ (Fig. 11). The temperature ($T$) dependence of the activation free energy $\Delta G = \Delta H - T\Delta S$ is also shown in Table IV. The activation free energy of the flip–flop motion per single hydrogen bond is $10.5–10.9\,\mathrm{kJ\,mol^{-1}}$. The decomposition to $T\Delta S$ and $\Delta H$ makes clear that the enthalpic term is larger than the entropic one.

## Comparison with Calix[4]arenes and Calix[6]arenes

The aim of this study is characterization of thiacalix[4]arene with respect to the "classical" compound, calix[4]arene, to give some hints for designing new supramolecular structures. Very recently we found that the activation parameters of calix[4]arene to be $\Delta G = 44.8–47.7\,\mathrm{kJ\,mol^{-1}}$, $\Delta S = -35\,\mathrm{J\,K^{-1}\,mol^{-1}}$, $\Delta H = 36.8\,\mathrm{kJ\,mol^{-1}}$ [8], which suggests that the flip–flop rates in thiacalix[4]arene are slightly higher. Interestingly, while the activation enthalpies are rather similar, there is a substantial difference in the activation entropies, which is the major cause of lower hydrogen bond array stability in thiacalix[4]arene.

The interrelation of the activation entropy difference and the structural properties turns out to be fairly complex. We attempted the B3LYP/6-31G** calculations of the enthalpies and entropies (evaluated within the rigid rotor—harmonic oscillator—ideal gas approximations) of the ground state and the transition state (in which all four hydrogen atoms are placed symmetrically between the donor and acceptor oxygens), but it did not lead to agreement with the experimental data (values not shown). Therefore, hard-core quantum chemical calculations will have to be performed. The mechanism of the flip–flop process is probably more complicated, e.g. multi-step. The influence of the solvent cannot be omitted either. Such unequal interaction of the "classical" and thiacalix[4]arenes with a solvent was previously reported in the case of the lower rim substituted compounds (tetramethyl-, tetraethyl-) that display different rates of the *pinched cone–pinched cone* interconversion (these compounds adopt the "pinched" $C_{2v}$ geometry rather than apparent $C_{4v}$ as in the case of the unsubstituted ones). The proposed explanation was stabilization of the $C_{4v}$ symmetrical transition state of the thiacalix[4]arene derivatives due to interaction with solvent [29].

Meanwhile, we compare the *ab initio* calculated structural parameters of hydrogen bond arrays in thiacalix[4]arene and calix[4]arene with the experimentally determined parameters (Table V). It is interesting to note that oxygen atoms in the two structures in Fig. 12 are superimposed rather well, and the slightly larger size of thiacalix[4]arene macrocycle is responsible for the O–H–O bond angle being smaller for 12.5 degrees. The calix[4]arene macrocycle thus seems to be somewhat better preorganized for the lower rim hydrogen bonding. However, it is not clear why should be the geometrical features transmitted into the different

TABLE V Comparison of experimentally and theoretically (*ab initio* calculations) obtained properties of hydrogen bonds arrays of thiacalix[4]arene and calix[4]arene (values taken from ref. [8]). The activation enthalpy of the flip–flop $\Delta H$, the activation entropy of the flip–flop $\Delta S$, and the $^1H$ chemical shift of hydroxyl groups $\delta_{OH}$ are determined experimentally, while the distance between the oxygen atoms of adjacent phenyl units and the O–H—O bond angle are taken from the calculated structures.

| | $\Delta H/(\mathrm{kJ\,mol^{-1}})$ | $\Delta S/(\mathrm{J\,mol^{-1}\,K^{-1}})$ | $\delta_{OH}$/ppm | O–O distance/pm | O–H–O bond angle/deg |
|---|---|---|---|---|---|
| Thiacalix[4]arene | 38.7 | − 15 | 9.6 | 274.9 | 152.1 |
| Calix[4]arene | 36.8 | − 35 | 10.2 | 264.5 | 164.6 |

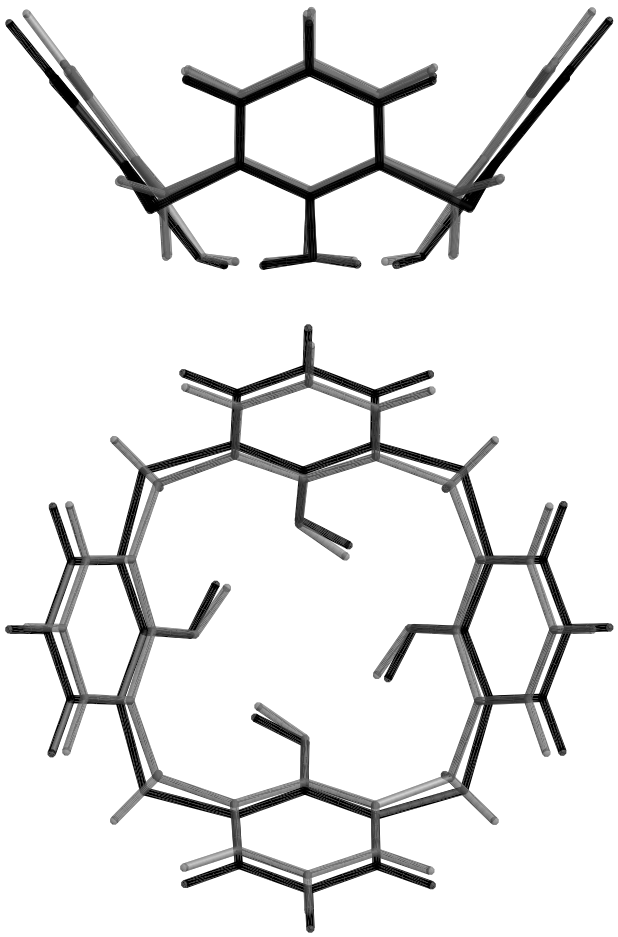

FIGURE 12 Comparison of thiacalix[4]arene (black) and calix[4]arene (grey) *ab initio* calculated structures.



activation entropies rather than the enthalpies.

Our results are in accord with Kovalenko *et al*. [30] who studied the two molecules by means of IR and UV/VIS spectroscopy. The measured frequencies of the OH stretching vibration were $3310\,cm^{-1}$ for thiacalix[4]arene and $3173\,cm^{-1}$ for calix[4]arene (in $CCl_4$ solutions) thus documenting a very strong hydrogen bonding in calix[4]arene and somewhat weaker one in the *thia* analogue. The authors suggested that differences between the two molecular systems could be caused by the different sizes of their macrocycles and by two additional effects: (i) bifurcated hydrogen bonds in thiacalix[4]arene (towards the neighboring oxygen and the bridging sulfur), and (ii) the electron density transfer from the sulfur bridges towards the benzene rings. The occurrence of the latter effect was supported by the measured UV spectra [30].

There is one more interesting difference apparent when comparing the two compounds. Rotational correlation times of the two molecules as obtained from the motional analysis display the values for thiacalix[4]arene systematically smaller than those for calix[4]arene, although the first one is slightly larger and heavier. There are two possible explanations, namely, the interaction with solvent and/or a certain degree of internal mobility in thiacalix[4]arene. The internal motions would not be correctly treated by the model of isotropic reorientation of a solid sphere, which would result in effective shortening of the obtained correlation times. Unfortunately, distinguishing between these two options is not readily possible. In order to determine whether the local motion indeed occurs one could, in principle, measure the spin relaxation at several magnetic fields. Clearly, the faster motion would be better determined at higher magnetic field(s). However, the main problem lies in simultaneous action of the two relaxation mechanisms—the DD interactions and the CSA, with the CSA amplitude proportional to the square of applied magnetic field. The accuracy of determination of the amplitudes of the two interactions is limited, and this uncertainty propagates further, because the relaxation rates are proportional to the squares of the amplitudes. Our model calculation showed roughly 10% difference in the expected longitudinal relaxation rates with or without the local motion at magnetic field of 20 T. This difference can easily be masked by the existing uncertainties in the interaction amplitudes. In addition, previous measurements did not suggest an internal motion of the thiacalix[4]arene macrocyclic core on the picosecond timescale [13]. The current observation can be, perhaps, better explained by the formation of an adduct of calix[4]arene with the chlorinated solvent that slows down its tumbling.

We do not take into account the *cone–inverted cone* transition in the current analysis, because it is not possible to establish its rate in thiacalix[4]arene experimentally due to the replacement of the methylene bridging groups by sulfur. Nevertheless, we assume that this motion occurs roughly on the same time-scale as in the "classical" calix[4]arene. As a consequence, it affects neither the hydrogen bond flip–flop motion nor the molecular tumbling, both of these motions being much faster than the *cone–inverted cone* transition.

Another example of circular array of hydrogen bonds was described in a thorough study of conformational flexibility of calix[6]arenes by Molins *et al*. [31]. The authors found that 5,17,29-tri-*tert*-butyl-11,23,35-trichlorocalix[6]arene adopts a "winged" cone conformation, which can be related to the "pinched" cone in the case of calix[4]arenes—two opposite rings become close to the plain of the bridging atoms between the aromatic rings while the remaining ones become close to perpendicular to the plain. Thus, the molecule contains a cyclic array of six hydrogen bonds that are all non-equivalent in $^1H$ NMR spectrum at lower temperature (183 K). The reversal of the array could, therefore, be studied by

means of exchange spectroscopy that provided the free activation energy of 44.4 kJ mol$^{-1}$ [31], i.e. 7.4 kJ mol$^{-1}$ per single hydrogen bond. The total was nearly the same as the value received for calix[4]arene [8], and thus, the activation energy of the reversal per single bond was larger in calix[4] arene, roughly 1.5 times.

Arrays of 2–5 hydrogen bonds of different sizes were previously also observed and characterized in phosphates and thiophosphates of calix[6]arene and thiacalix[6]arene [32]. The lack of symmetry allowed the authors to distinguish all hydroxyl groups in the $^1$H NMR spectra and utilize the exchange spectroscopy. The free activation energies per single hydrogen bond were found to be 7.8–9 kJ mol$^{-1}$.

The average activation energy per single hydrogen bond determined here for thiacalix[4]arene is somewhat lower than for "classical" calix[4]arene and, conversely, for ca. 2–3 kJmol$^{-1}$ larger than in above mentioned calix[6]arenes. This feature can be ascribed to higher symmetry of the array and substantially lower internal mobility of the (thia) calix[4]arenes.



## METHODS

### Calculations

The geometry of thiacalix[4]arene was fully optimized employing the DFT B3LYP (Becke's three parameter exchange [33] and Lee, Yang, Parr correlation functionals [34]) and the standard 6-31G** basis set. The $C_4$ symmetry was exploited. The Gaussian 98 suite of programs [35] was used with default settings. The structural details can be inferred from the geometry of the optimized structure, which is included in the supplementary material in *xyz* format [28].

The $^{13}$C NMR CSTs were obtained using the SOS–DFPT–IGLO method as implemented in the deMon-MASTER-CS code [36,37]. The SOS–DFPT–IGLO strategy combines the sum-over-states density functional (Rayleigh–Schrödinger) perturbation theory with the individual gauges for localized (molecular) orbitals [38]. The IGLO-III basis set of Kutzelnigg *et al.* [38] (roughly of quadruple-ξ quality with two sets of polarization functions), the Perdew–Wang-91 exchange-correlation potential [39,40], the FINE angular integration grid with 64 radial shells [41], and the approximation Loc. 1 SOS-DFPT [42] were applied. The molecular orbitals were localized by the method of Boys [43].

### Experimental

A sample of 2,8,14,20-tetrathiacalix[4]arene was prepared according to the previously described procedure [9–11]. For the liquid state measurements, it was dissolved in 1,1,2,2-tetrachloroethane-$d_2$ (Chemotrade, 99.8% d) in the concentration of 0.03 mol/dm$^3$ (saturated solution). The sample was degassed by three times repeating the freeze-pump-thaw procedure and flame-sealed in 5 mm NMR tube. The liquid state NMR spectra were acquired on Bruker Avance 500 spectrometer operating at the magnetic field of 11.7 T. Experiments were performed at temperatures ranging from 193 K to 313 K. The instrument was equipped with the BVT-3000 temperature control unit and the thermocouple was calibrated using the methanol standard (Wilmad). The calibration was accurate to 0.2 K and temperature stability was better than 0.1 K. The temperature stability dropped to 0.2 K in some cases of very long (seconds) $\pi$-pulse trains that caused certain heating of the sample. The insufficient signal/noise ratio at the lowest temperatures (193–213 K) did not allow the relaxation measurements and only basic 1D spectra could be acquired.

The $^1$H spectra were acquired with the spectral width of 6 kHz, 32 K data points. The $\pi/2$ $^1$H pulse durations were between 13.1 and 14.3 μs.

The $^{13}$C spectra were acquired with the spectral width of 10 kHz–32 k data points. The $\pi/2$ $^{13}$C pulse durations were between 6.6 and 7.1 μs. The $^1$H decoupling or steady state NOE build-up were achieved by the Waltz-16 sequence on the power level corresponding to 100 μs $\pi/2$ pulse.

The $^{13}$C longitudinal relaxation was measured using the fast inversion recovery pulse sequence [44]. The relaxation delay was always set to be longer than $3 \times T_1$. At least 6 dummy scans preceded measurements for each value of the mixing time in order to establish a steady state of the nuclear magnetization prior to each pulse sequence run with data acquisition. The heteronuclear steady state $^{13}$C–{$^1$H} NOE was measured using the dynamic NOE sequence [45]. In the first run, the sequence contained the $^1$H irradiation period $5 \times T_1$ long, in the second run, this period was removed. The relaxation period was always set to take longer than $8 \times T_1$. The NOE was evaluated as the ratio of signal intensities of the two runs.

The transverse relaxation was measured using the CPMG pulse sequence [18] with $^1$H $\pi$-pulses added to remove cross-correlation between CSA and DD interactions [17]. For all temperatures, an experiment with fixed echo-time ($t_{echo}$) set to 0.8 ms was performed to measure transverse relaxation rates $R_2$. In addition, other experiments with variable $t_{echo}$ were carried out to assess also the chemical exchange rate—either several separate $T_2$ measurements for different $t_{echo}$ values, or the "accelerated" experiments [19] when $n$ and $t_{echo}$ were varied synchronously, so that $nt_{echo} = 20$, 30 or 100 ms (see Table VI). The lower bound of $t_{echo}$ was imposed by the shortest transmitter duty cycle and by the need to

TABLE VI Experimental settings of the transverse relaxation measurements (CPMG) performed.

| $T$/K | CPMG-$T_2$ measurement $t_{echo}$/ms | CPMG-"accelerated" experiment $nt_{echo}$/ms |
|---|---|---|
| 223 | 0.2; 0.4; 0.8; 1.2; 1.6; 2.0; 3.0 | – |
| 233 | 0.8 | 20; 30 |
| 243 | 0.8 | 20 |
| 253 | 0.8 | 20; 30 |
| 263 | 0.8 | 20 |
| 273 | 0.2; 0.4; 0.6; 0.8; 1.0; 1.2; 1.6; 2.4; 3.2; 4.0 | – |
| 283 | 0.8 | – |
| 293 | 0.8 | – |
| 303 | 0.2; 0.8 | – |
| 313 | 0.8 | 100 |

prevent excessive sample heating, while the upper bound was restricted by the required accuracy of the $T_2$ determination, since for the long echo-times, only a few values of the mixing time were available before the magnetization decayed. The number of mixing time increments thus varied between 10 and 14. The relaxation delay was set to be $5 \times T_1$.

Relaxation times were calculated from the dependences of the line intensities on the mixing time by three ($T_1$) or two ($T_2$) parameter fitting of exponential functions using the spectrometer software.

All other calculations were performed applying our routines written in Matlab 6. The errors of the calculated quantities were estimated by means of the Monte Carlo simulations. New virtual datasets (typically 100) for each fitting routine were created in such a way that the new data points were generated according to the normal distribution around the experimental value. The variance of the distribution was set to be the same as the standard deviation of the particular fit. The standard deviations of the results of the fittings the simulated datasets were taken as the standard error of the particular parameter determination.

The variances in the case of calculation of the correlation time from $T_1$, $T_2$ and NOE were 5% except for $T_1$ of C-3, C-5 and C-4 (2.5%) that correspond to the conservatively estimated experimental errors. Standard deviations of the fits of $T_1$ and $T_2$ from the experimental signal intensities were always lower.

The solid state $^{13}C$ measurements were carried out on a Chemagnetics Infinity-400 spectrometer operating at the magnetic field of 9.4 T. About 100 mg of thiacalix[4]arene was placed into 4 mm rotor. The spectra for determination of the CST were acquired using 2D PASS sequence [21] synchronized with the magic angle spinning at 1.5 kHz. The measurements were carried out at the temperature of 233 K. The $^{13}C$ $\pi/2$ pulse duration was 2 μs, the cross-polarization period was 7 ms. The intensities of the rotational sidebands were obtained by integration of the resonances in each row of the PASS spectrum. They were fitted to Herzberg–Berger formula using the program HBA [22] in order to obtain the CST principal components. Because no chemical shift standard was used in the solid-state measurements, the isotropic chemical shifts from the liquid-state spectrum at 233 K (relative to TMS) were used as the central band frequency for the fitting.

## CONCLUSIONS

The hydrogen bond array in thiacalix[4]arene in a non-polar solution undergoes a flip–flop motion with the rates spanning from $7{\cdot}10^2$ to $5{\cdot}10^5\,s^{-1}$ in the temperature range 223–313 K. The corresponding activation enthalpy is $38.6\,kJ\,mol^{-1}$ and the activation entropy is $-15\,J\,mol^{-1}\,K^{-1}$. The comparison with calix[4]arene reveals that the hydrogen bond array in thiacalix[4]arene is for $2–4\,kJ\,mol^{-1}$ less stable, the major difference being in the entropic term ($-35\,J\,mol^{-1}\,K^{-1}$ in calix[4]arene).

The correlation time of molecular tumbling was determined to lie in the interval from 1.9 to 0.072 ns over the temperatures ranging from 223–313 K. Surprisingly, this is shorter than in the previously studied calix[4]arene. Possible explanations are some degree of internal mobility of thiacalix[4]arene on the picosecond timescale and/or different interactions with solvent. Unfortunately, current methods do not allow us to distinguish between these two options.

### *Acknowledgements*

Financial supports from the Czech Science Foundation (Grant. No 203/04/P168 to JL) and from the Grant Agency of the Czech Academy of Sciences (Grant No. KJB5040311 to JC and JL) are gratefully acknowledged. This work is a part of the research plan MS 0021620835 that is financed by the Ministry of Education of the Czech Republic. J.C. appreciates generous allotment of computer time in the Czech Academic Supercomputer Centre and in the Mississippi Center for Supercomputing Research. J.L. is indebted to Dr Sergei Dvinskikh from Stockholm University for his kind assistance in operating the solid state NMR spectrometer.

### *References*

[1] Gutsche, C. D. In *Calixarenes; Monographs in Supramolecular Chemistry*; Stoddart, J. F., Ed.; The Royal Society of Chemistry: Cambridge, 1989.
[2] Gutsche, C. D. In *Calixarenes Revisited; Monographs in Supramolecular Chemistry*; Stoddart, J. F., Ed.; The Royal Society of Chemistry: Cambridge, 1998.
[3] Fischer, S.; Grootenhuis, P. D. J.; Groenen, L. C.; Hoorn, W. P.; van Veggel, F. J. C. M.; Reinhoudt, D. N.; Karplus, M. *J. Am. Chem. Soc.* **1995**, *117*, 1611–1620.
[4] Groenen, L. C.; van Loon, J.-D.; Verboom, W.; Harkens, S.; Casnati, A.; Ungaro, R.; Pochini, A.; Ugozzoli, F.; Reinhoudt, D. N. *J. Am. Chem. Soc.* **1991**, *113*, 2385–2392.

[5] van Hoorn, W. P.; Briels, W. J.; van Duynhoven, J. P. M.; van Veggel, F. J. C. M.; Reinhoudt, D. N. *J. Org. Chem.* **1998**, *63*, 1299–1308.
[6] Groenen, L. C.; Steinwender, E.; Lutz, B. T. G.; van der Maas, J. H.; Reinhoudt, D. N. *J. Chem. Soc. Perkin Trans.* **1992**, *2*, 1893–1898.
[7] Grootenhuis, P. D. J.; Kollman, P. A.; Groenen, L. C.; Reinhoudt, D. N.; van Hummel, G. J.; Ugozzoli, F.; Andreetti, G. D. *J. Am. Chem. Soc.* **1990**, *112*, 4165–4176.
[8] Lang, J.; Deckerová, V.; Czernek, J.; Lhoták, P. *J. Chem. Phys.* **2005**, *122*, 044506.
[9] Akdas, H.; Bringel, L.; Graf, E.; Hosseini, M. W.; Mislin, G.; Pansanel, J.; DeCian, A.; Fischer, J. *Tetrahedron Lett.* **1998**, *39*, 2311–2314.
[10] Iki, N.; Kabuto, C.; Fukushima, T.; Kumagai, H.; Takeya, H.; Miyanari, S.; Miyashi, T.; Miyano, S. *Tetrahedron* **2000**, *56*, 1437–1443.
[11] Sone, T.; Ohba, Y.; Moriya, K.; Kumada, H.; Ito, K. *Tetrahedron* **1997**, *53*, 10689–10698.
[12] Canet, D. *Nuclear Magnetic Resonance: Concepts and Methods*; John Wiley & Sons: Chichester, 1996.
[13] Lang, J.; Tošner, Z.; Lhoták, P.; Kowalewski, J. *Magn. Reson. Chem.* **2003**, *41*, 819–827.
[14] Antony, J. H.; Dölle, A.; Fliege, T.; Geiger, A. *J. Phys. Chem. A* **1997**, *101*, 4517–4522.
[15] Shultes, M.; Eisenhauer, R.; Dechter, J. J.; Johansson, M.; Kumar, P.; Kowalewski, J. *Magn. Reson. Chem.* **1999**, *37*, 799–804.
[16] Luz, Z.; Meiboom, S. *J. Chem. Phys.* **1964**, *39*, 366.
[17] Kay, L. E.; Nicholson, L. K.; Delaglio, F.; Bax, A.; Torchia, D. A. *J. Magn. Reson.* **1992**, *97*, 359.
[18] Meiboom, S.; Gill, D. *Rev. Sci. Instrum.* **1958**, *29*, 688.
[19] Ishima, R.; Baber, T.; Louis, J. M.; Torchia, D. A. *J. Biomol. NMR* **2004**, *29*, 187–198.
[20] Kowalewski, J.; Effemey, M.; Jokisaari, J. *J. Magn. Reson.* **2002**, *157*, 171–177.
[21] Antzutkin, O. *Prog. NMR Spectrosc.* **1999**, *35*, 203–266.
[22] Eichele, K.; Wasylishen, R. E. *HBA 1.4*; Dalhousie University: Halifax, 2001.
[23] Helgaker, T.; Jaszuński, M.; Ruud, K. *Chem. Rev.* **1999**, *99*, 239–352.
[24] Czernek, J.; Sklenář, V. *J. Phys. Chem. A* **1999**, *103*, 4089–4093.
[25] Czernek, J. *J. Phys. Chem. A* **2001**, *105*, 1357–1365.
[26] Fiala, R.; Czernek, J.; Sklenář, V. *J. Biomol. NMR* **2000**, *16*, 291–302.
[27] Jameson, A. K.; Jameson, C. J. *Chem. Phys. Lett.* **1987**, *134*, 461–466.
[28] see Supplementary Material for the tables of the measured relaxation rates, the tables of experimental spectral intensities of C-2, C-6 used for quantification of the chemical exchange rates and the *ab initio* computed structure of thiacalix[4]arene (*xyz*-coordinates). It is available from http://physics.mff.cunicz/kFNT/Nmr/download
[29] Čajan, M.; Lhoták, P.; Lang, J.; Dvořáková, H.; Stibor, I.; Koča, J. *J. Chem. Soc. Perkin Trans.*, *2*, **2002**, 1922–1929.
[30] Kovalenko, V. I.; Chernova, A. V.; Borisoglebskaya, E. I.; Katsyuba, S. A.; Zverev, V. V.; Shagidullin, R. R.; Antipin, I. S.; Solov'eva, S. E.; Stoikov, I. I.; Konovalov, A. I. *Russ. Chem. Bull.* **2002**, *51*, 825–827.
[31] Molins, M. A.; Nieto, P. M.; Sánchez, C.; Prados, P.; de Mendoza, J.; Pons, M. *J. Org. Chem.* **1992**, *57*, 6924–6931.
[32] Janssen, R. G.; van Duynhoven, J. P. M.; Verboom, W.; van Hummel, G. J.; Harkema, S.; Reinhoudt, D. N. *J. Am. Chem. Soc.* **1996**, *118*, 3666–3675.
[33] Becke, A. D. *J. Chem. Phys.* **1993**, *98*, 5648.
[34] Lee, C.; Yang, W.; Parr, R. *Phys. Rev. B* **1998**, *37*, 785.
[35] Frish, M. J. *et al. Gaussian 98, Revision A7*; Gaussian, Inc.; Pittsburg, 1998.
[36] Malkin, V. G.; Malkina, O. L.; Salahub, D. R. *MASTER-CS Program*; Universite de Montreal: Montreal, 1994.
[37] Salahub, D. R.; Fournier, R.; Mlynarski, P.; Papai, A.; St-Amant, A.; Uskio, J. In *Density Functional Methods in Chemistry*; Labanowski, J., Adzhelm, J. W., Eds.; Springer: New York, 1991; p 77.
[38] Kutzelnigg, W.; Fleischer, U.; Schindler, M. *NMR Basic Principles and Progress*; Springer-Verlag: Berlin, 2000; 23, p 165.
[39] Perdew, J. P.; Wang, Y. *Phys. Rev. B* **1992**, *45*, 13244.
[40] Perdew, J. P.; Chevary, J. A.; Vosko, S. H.; Jackson, K. A.; Pederson, M. R.; Singh, D. J.; Fiolhais, C. *Phys. Rev. B* **1992**, *46*, 6671.
[41] Malkin, V. G.; Malkina, O. L.; Eriksson, L. A.; Salahub, D. R.; Seminario, J. M.; Politzer, P. *Theoretical and Computational Chemistry*; Elsevier: Amsterdam, 1995; Vol. 2, pp 273–347.
[42] Malkin, V. G.; Malkina, O. L.; Casida, M. E.; Salahub, D. R. *J. Am. Chem. Soc.* **1994**, *116*, 5898–5908.
[43] Boys, S. F. In *Quantum Theory of Atoms, Molecules, and the Solid State*; Löwdin, P.-O., Ed.; Academic Press: New York, 1969; p 263.
[44] Canet, D.; Levy, G. C.; Peat, I. R. *J. Am. Chem. Soc.* **1975**, *18*, 199–204.
[45] Kowalewski, J.; Ericsson, A.; Vestin, R. *J. Magn. Reson.* **1978**, *31*, 165.